Article

Current Biology

Suppression of motion vision during course-changing, but not course-stabilizing, navigational turns

Highlights

- Optic-flow processing neurons are suppressed during loom-evoked flight turns
- This suppression cuts signaling of head-movement-induced visual motion during turns
- The cells are not suppressed during optomotor responses to rotational visual motion
- Suppression thus occurs during course-changing, but not course-stabilizing, turns

Authors

Lisa M. Fenk, Anmo J. Kim, Gaby Maimon

Correspondence

lfenk@neuro.mpg.de (L.M.F.), anmokim@hanyang.ac.kr (A.J.K.), maimon@rockefeller.edu (G.M.)

In brief

Fenk et al. show that optic-flow processing neurons have their activity suppressed during course-changing, but not course-stabilizing, navigational turns. Such contextual, motor-related suppression makes sense for neurons whose visual responses normally serve to help an animal maintain a consistent navigational trajectory or gaze angle.

Fenk et al., 2021, Current Biology *31*, 4608–4619
October 25, 2021
https://doi.org/10.1016/j.cub.2021.09.068

CellPress

CellPress
OPEN ACCESS

Current Biology

Article

Suppression of motion vision during course-changing, but not course-stabilizing, navigational turns

Lisa M. Fenk,[1,2,5,*] Anmo J. Kim,[1,3,4,5,*] and Gaby Maimon[1,6,*]
[1]Laboratory of Integrative Brain Function and Howard Hughes Medical Institute, The Rockefeller University, New York, NY, USA
[2]Active Sensing, Max Plank Institute of Neurobiology, Martinsried, Germany
[3]Department of Biomedical Engineering, Hanyang University, Seoul, South Korea
[4]Department of Electronic Engineering, Hanyang University, Seoul, South Korea
[5]These authors contributed equally
[6]Lead contact
*Correspondence: lfenk@neuro.mpg.de (L.M.F.), anmokim@hanyang.ac.kr (A.J.K.), maimon@rockefeller.edu (G.M.)
https://doi.org/10.1016/j.cub.2021.09.068

SUMMARY

From mammals to insects, locomotion has been shown to strongly modulate visual-system physiology. Does the manner in which a locomotor act is initiated change the modulation observed? We performed patch-clamp recordings from motion-sensitive visual neurons in tethered, flying *Drosophila*. We observed motor-related signals in flies performing flight turns in rapid response to looming discs and also during spontaneous turns, but motor-related signals were weak or non-existent in the context of turns made in response to brief pulses of unidirectional visual motion (i.e., optomotor responses). Thus, the act of a locomotor turn is variably associated with modulation of visual processing. These results can be understood via the following principle: suppress visual responses during course-changing, but not course-stabilizing, navigational turns. This principle is likely to apply broadly—even to mammals—whenever visual cells whose activity helps to stabilize a locomotor trajectory or the visual gaze angle are targeted for motor modulation.

INTRODUCTION

Motor signals modulate sensory physiology in varied brain regions and during diverse actions, from the twitching of facial muscles to the act of locomotion.[1–5] A deeper understanding of the function of these motor-related modulations would be an important step forward for systems neuroscience.

An intriguing aspect of motor control is that the same physical movement can serve different functions depending on context. Consider, for example, a person jogging in nature. This individual is likely to make many internally initiated or spontaneous navigational turns as they explore their new environment. They might also turn rapidly away from a looming object, like an elevated boulder tumbling toward them. Both the spontaneous and loom-evoked turns can be considered course-changing in that their purpose is to alter the navigational trajectory. On the other hand, a very strong gust of wind might come and cause this person's body to rotate during the jog, which might then drive them to quickly turn back toward their initial direction of travel. Such turning-back behavior is a course-stabilizing turn in that its purpose is to help maintain a consistent navigational trajectory after an unexpected perturbation. Should we expect this person's visual system to be modulated the same way during all the above-mentioned turns—if the kinematics were generally matched—or might course-changing and course-stabilizing navigational turns lead to different modulations because their behavioral purpose is different? Answering this question might illuminate at least some of the reasons why sensory physiology is so pervasively modulated by movement.

We studied modulations of visual signaling in the *Drosophila* gaze control system during tethered flight. Flying flies intersperse periods of straight flight (or hovering) with quick turns, called saccades. We previously reported on motor-related signals in optic-flow processing neurons whose sign, timing, and magnitude are appropriate for silencing the expected visual responses of those neurons during rapid flight turns.[6,7] To date, however, these motor-related signals have only been observed during spontaneous saccades, which are course-changing turns that occur at unpredictable times relative to any measurable external event.[8–11] Many locomotor turns in flies, however, are evoked by visual stimuli.[8,12,13]

In this study, we compare motor-related signals in optic-flow processing neurons during spontaneous flight turns with those observed during two types of visually driven turns: loom-evoked and optomotor (Figures 1A and 1B). In loom-evoked turns, flies rapidly turn away from an expanding disc. In optomotor responses, flies turn in the direction of rotational visual motion. Loom-evoked turns are course-changing and reflect an attempt by the fly to evade an approaching object. Optomotor responses are course-stabilizing because they reflect corrective turns that help to maintain a consistent gaze or traveling angle. We observed motor-related inputs to optic-flow processing neurons during loom-evoked flight turns, akin to our original observations during spontaneous turns, but we could not detect motor-related

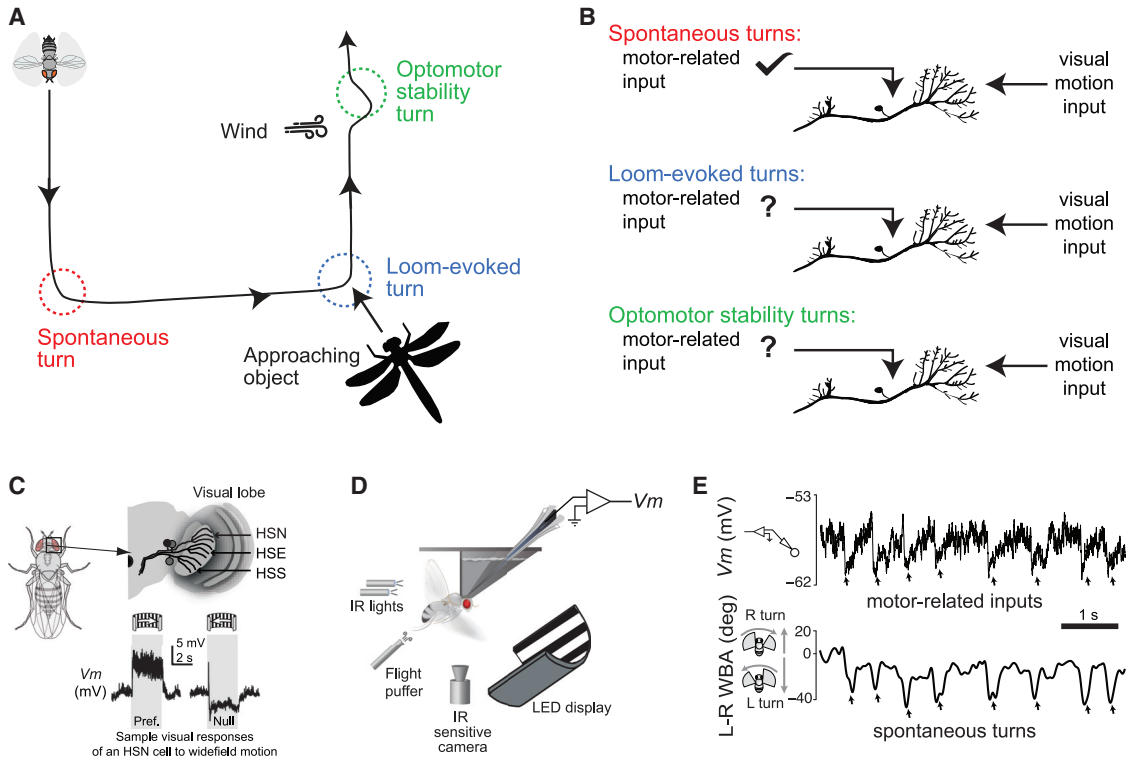

Figure 1. Course-changing and course-stabilizing flight turns and motor-related inputs to the horizontal system (HS) cells

(A) Schematic of different types of flight turns.

(B) We will test the hypothesis that loom-evoked and optomotor turns are associated with motor-related input to HS cells.

(C) Top: fly visual lobe with HS cells schematized. Bottom: a sample recording of an HSN cell in the right lobula plate responding to clockwise (preferred direction) and counter-clockwise (null direction) panoramic visual motion.

(D) Setup for patch-clamp recordings in tethered, flying *Drosophila* and tracking of wing-steering behavior.

(E) Example membrane potential (*Vm*) trace from an HSN cell in the right lobula plate (top) and the concomitant left-minus-right wingbeat amplitude (L-R WBA) wing-steering trace (bottom) in the context of a uniformly lit screen. Spontaneous turns/saccades (arrows, bottom) coincide with saccade-related potentials (arrows, top).

inputs during optomotor responses. The simplest interpretation is that the motor-related inputs in this system act to suppress the visual activation of these cells during course-changing, but not course-stabilizing, navigational turns. This interpretation—based upon the magnitude of motor-related signals during different modes of action initiation—generally supports the notion that these inputs function as efference copies, as classically defined,[14,15] consistent with past interpretations based on other lines of evidence.[6] Comparing the magnitude of motor-related signals across modes of action initiation may be a general way, even beyond insects, to gain insight into the function of motor-related modulations in varied visual systems.

RESULTS

Optic-flow processing neurons show transient membrane potentials during loom-evoked flight turns

We studied motor-related signals in the horizontal system (HS) cells of the fly's optic lobe[16–18] during course-changing and course-stabilizing flight turns (Figures 1A and 1B). HS cells are large visual interneurons located in the lobula plate, four synapses downstream of photoreceptors. There are three uniquely identifiable horizontal system cells in each lobula plate: the horizontal system north (HSN) cell, horizontal system equatorial (HSE) cell, and the horizontal system south (HSS) cell (Figure 1C). These three cells anatomically span the top, middle, and bottom part of the lobula plate and, correspondingly, their receptive fields span the ipsilateral dorsal, middle, and ventral fields of view, respectively.[16,17] All three HS cell types show direction-selective responses to visual motion, and they are particularly sensitive to panoramic, wide-field motion, called optic flow. HS cells on the right side of the fly brain are depolarized by clockwise rotational visual motion (preferred direction) and they are hyperpolarized by counterclockwise motion (null direction) (Figure 1C). HS cells on the left side show the opposite tuning.

By performing whole-cell patch-clamp recordings from HS cells in tethered, flying *Drosophila* (Figure 1D), we previously showed that these neurons, in addition to their classic visual responses, receive motor-related inputs during rapid flight turns or saccades. We can detect spontaneous saccades as quick deviations in the left-minus-right wingbeat amplitude (L–R WBA) behavioral signal[6,7] (Figure 1E, arrows, bottom trace). The motor-related inputs are evident as saccade-related potentials (SRPs) that hyperpolarize HS cells on the right side during

leftward turns (Figure 1E, arrows, top trace), and vice versa, which is the appropriate sign if SRPs are to suppress the expected visual activation of HS neurons during a turn. To date, however, SRPs have only been described in the context of spontaneous saccades. Are SRPs also evident in HS cells during sensory-evoked turns, in particular during rapid evasive maneuvers made in response to looming visual objects?

In preliminary experiments, we performed patch-clamp recordings from HS cells while presenting looming stimuli in the context of an otherwise uniformly lit (i.e., blank) screen. Whereas HS cells showed membrane potential (*Vm*) modulations to the looming stimuli, we could not definitively determine whether the signals reflected visual responses to the expanding disc or motor-related potentials to the saccade (data not shown). HS cells are tuned to rotational motion, but they also activate to an expanding-disc stimulus, albeit more weakly. One of the main challenges in dissociating visual and motor contributions in these initial experiments was that SRPs tend to be small, and thus hard to detect, in the absence of depolarizing visual drive.[6]

We therefore modified our stimulus to increase the size of SRPs. We previously discovered that hyperpolarizing SRPs grow in magnitude when HS cells are tonically depolarized by visual motion, either because the saccade-related conductance is actively strengthened in this context or because the HS cells' *Vm* is further away from the reversal potential of a consistent saccade-related conductance.[6] We thus presented looming stimuli in the context of a widefield motion stimulus that tonically depolarized HS cells. Specifically, we recorded from HS cells in the right lobula plate and depolarized them with a set of bars (a square-wave grating) rotating clockwise on the contralateral side of the screen, extending 54° into the ipsilateral side. During loom trials, we additionally presented a looming disc on the ipsilateral side (Figure 2A; Video S1; STAR Methods). We also included no-loom trials, which were identical to loom trials except that the disc never expanded (Figure 2A; Video S2).

In a typical loom trial, we observed that an HS cell tonically depolarized in response to the grating (Figure 2B, top) and the fly performed a slow, ramping optomotor response with her wings (Figure 2B, bottom, rising L–R WBA trace after grating motion onset). This rightward optomotor response was interspersed by frequent saccades to the left, as previously described,[9] which co-occur with large hyperpolarizing SRPs (Figure 2B, small arrows). These nystagmus saccades are reminiscent of the rapid, nystagmus eye movements that vertebrates make while performing an optokinetic response to a rotating grating.[18] Toward the end of the loom's expansion (shaded area), the fly performed the expected saccade away from the looming disc (Figure 2B, large arrow), and this saccade was associated with a *Vm* hyperpolarization that resembled the nystagmus-saccade SRPs.

The single trial was representative for all trials measured from this fly (Figure 2C). Nystagmus saccades largely averaged out in the mean behavioral trace, consistent with them having variable onset times relative to the onset of grating motion across trials (Figure 2C, bottom, thick line before loom). Because the occurrence times of nystagmus saccades are variable in relation to the onset of visual motion, we will consider them as "spontaneous" actions herein, but how one wishes to categorize these saccades is not essential for our main points. The behavioral response to the loom, on the other hand, remained visible in the average trace, alongside a concomitant *Vm* hyperpolarization. In principle, this hyperpolarization could reflect a feedforward visual response to the looming disc or a motor-related potential related to the act of turning. Which interpretation is most parsimonious?

Analyses leveraging trial-to-trial variability in behavioral responses argue that the loom-evoked modulation in HS cells has a strong motor-related component

To examine whether the loom-associated hyperpolarization was a motor-related signal, we took advantage of the fact that some flies (unlike the example fly in Figures 2B and 2C) showed significant trial-to-trial variability in their behavioral response to the loom. This meant that we could analyze whether the magnitude of the loom-associated potential correlated with the size of the variable behavioral response to the loom, which would be expected if the loom-associated potential were to reflect a motor-related signal.

In Figure 2D, we show two loom trials recorded in a fly that showed significant variability in her response to the expanding discs. A clear membrane hyperpolarization was evident on a trial in which the fly responded strongly to the loom (dark blue), but not on a trial where she responded weakly (light blue) (STAR Methods). We observed the same trend in averaged traces from trials with large behavioral responses to the loom (Figure 2E, right column, dark blue) and those with small behavioral responses to the loom (Figure 2E, right column, light blue). On trials with large behavioral responses, the average loom-associated potential grossly resembled the average nystagmus SRP (Figure 2E, red top trace). We observed that trials with small responses to the loom often tended to be those where the fly had just performed a spontaneous saccade immediately prior to the loom (e.g., light-blue saccade that begins right before the gray region in Figure 2D, marked by a light blue arrow), which might explain some of the variability in behavior. These pre-loom saccades on small response trials led to a lower L–R WBA and *Vm* baselines prior to the loom (light blue curves are lower than dark blue curves at baseline in Figure 2E), an issue we consider further below. Note that this observation means that L–R WBA and HS *Vm* were well correlated both before and throughout the time course of the response to the loom (Figures 2D and 2E).

We quantified the magnitude of behavioral responses on a trial-by-trial basis by first defining two 120-ms time windows. The first window began when the disc started expanding and extended forward 120 ms. This window was our baseline window because the flies were not yet responding during this time period. The second window started at the end of the first window and extended forward 120 ms. This window was our response window because the flies performed their loom-evoked turns in this time period. We quantified the magnitude of behavioral and neuronal responses on a trial-by-trial basis by subtracting the mean L–R WBA and *Vm*, respectively, in these time windows. In this fly, we found a strong linear relationship between behavioral and neuronal responses across trials (Figure 2F, $r = 0.92$, slope = 0.19 mV/deg). Such a correlation could arise if both neuronal and behavioral responses get weaker over time, due to adaptation/fatigue.[19] However, the fly alternated, trial-to-trial, between large and small turn responses (gray shading in Figure 2F reflects trial number, with darker points indicating later

CellPress
OPEN ACCESS

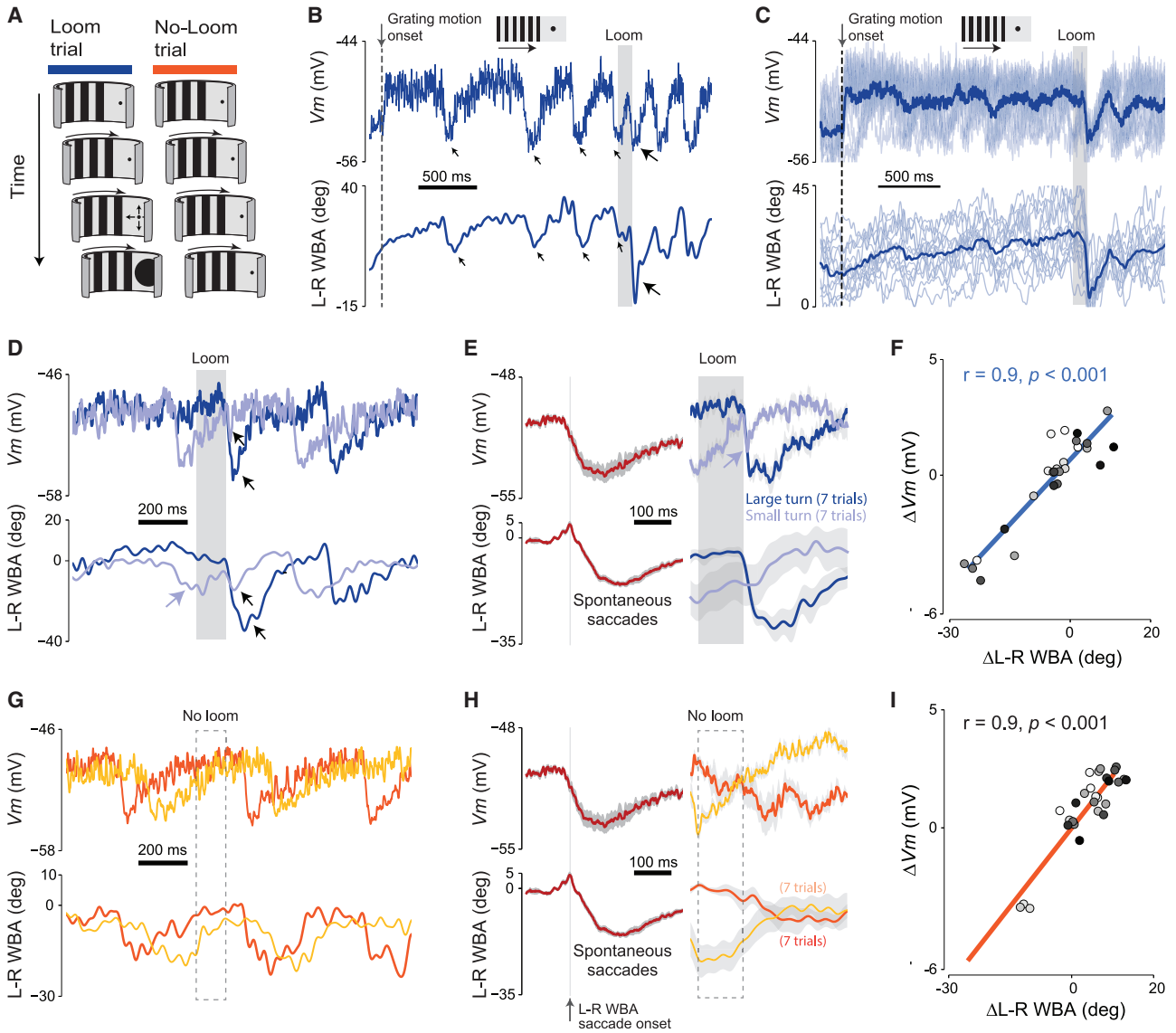

Figure 2. Single-cell analyses of motor-related inputs to HS cells during spontaneous and loom-evoked saccades

(A) Stimulus paradigm for HS cell recordings on the right side of the brain. After 2 s of clockwise grating motion a disc expands on the right (loom trials, Video S1). Trials without loom expansion served as a control (Video S2).

(B) Example *Vm* (top) and left-minus-right wingbeat amplitude (L–R WBA) (bottom) for a loom trial. Grating motion onset is indicated by a dotted vertical line. Disc expansion is indicated by the gray rectangle.

(C) Individual *Vm* and L–R WBA traces (light traces, n = 15 trials) together with the averages (dark blue).

(D) Individual trials from one fly showing strong (dark blue) and weak (light blue) behavioral responses (black arrows) to the loom (bottom) and concomitant changes in *Vm* (top).

(E) Left column shows the mean ± SEM spontaneous saccade (bottom) and SRP (top) during grating motion (n = 9 flies). Right column shows loom-aligned, trial-averaged data from strong loom-response trials (mean ± SEM, dark blue, n = 7 trials) and weak loom-response trials (light blue, n = 7 trials).

(F) Mean *Vm* change between the 120 ms following the loom and 120 ms preceding the loom plotted against the mean L–R WBA change in the same time windows. Shading of data points indicates trial number; darker points are trials that occurred later. Blue line: linear regression of scattered data.

(G–I) Example traces, averages, and Δ*Vm* to ΔL–R WBA relationship for no-loom trials as in (D)–(F). (H) Orange, n = 7 trials, yellow, n = 7 trials.

trials), arguing against any fatigue-related explanation for the observed correlation.

At face value, the high correlation between behavioral and neuronal responses during looms argues that motor-related inputs impact HS cell physiology during loom-evoked turns. However, a potential concern is that when we analyzed no-loom trials in the same manner, we observed a similar correlation (Figures 2G–2I). This result makes sense when one keeps in mind that flies were constantly performing spontaneous saccades. Thus, when testing any arbitrary time window, one expects to observe a correlation between *Vm* and L–R WBA due to the known relationship between *Vm* and L–R WBA for spontaneous

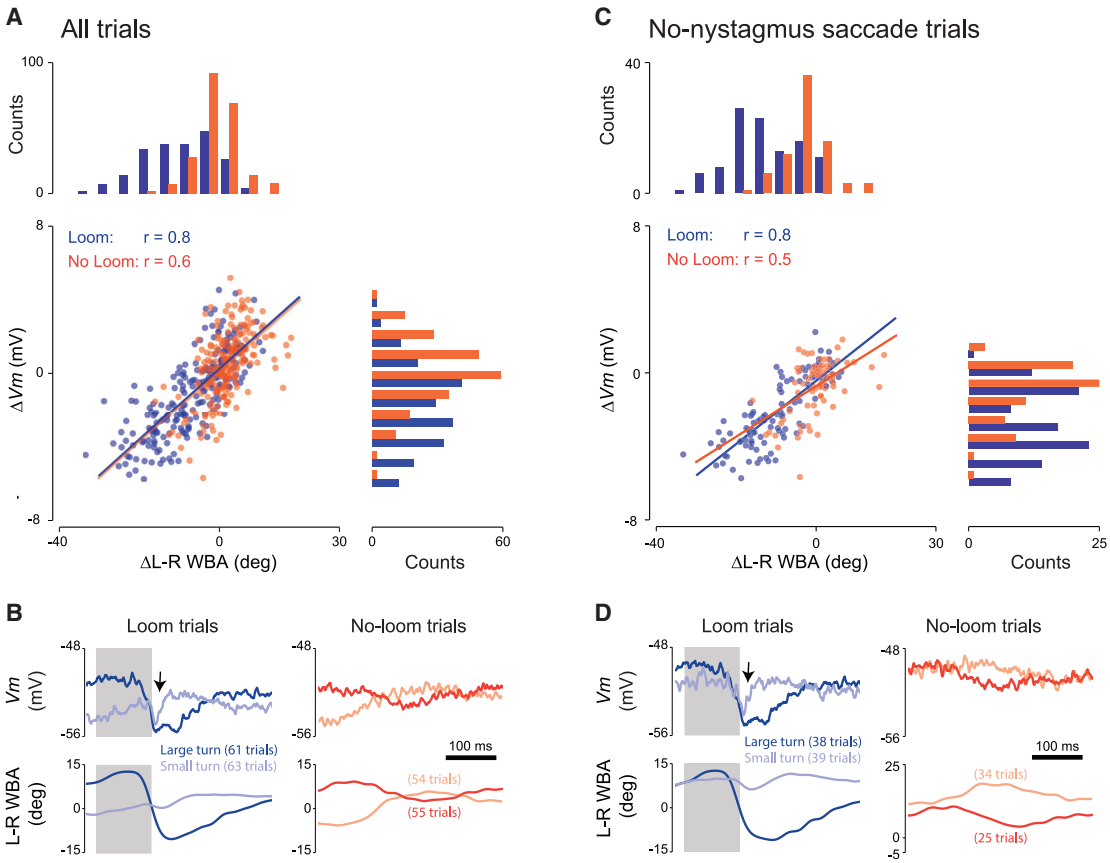

Figure 3. Population-level analyses of motor-related inputs to HS cells during spontaneous and loom-evoked saccades

(A) Change in *Vm* plotted against change in left-minus-right wingbeat amplitude (L–R WBA) (across the 120 ms before and after the end of the loom) for loom trials (blue, n = 211 trials) and no-loom trials (orange, n = 220 trials). One dot represents one trial; data from 9 flies are shown. Colored lines: linear fits ($p < 0.001$). Histograms of ΔL–R WBA (horizontal) and Δ*Vm* (vertical) for both stimulus conditions are shown.

(B) Average L–R WBA and *Vm* of loom trials with large turns (dark blue) and small turns (light blue). Average L–R WBA and *Vm* of no-loom trials with large turns (dark orange) and small turns (light orange).

(C) Same as (A) but for a subset of trials that met the no-nystagmus-saccade criterion (n = 104 loom trials, n = 77 for no-loom trials). $p < 0.001$ for both linear fits.

(D) Same as (B) but for the subset of trials that met the no-nystagmus-saccade criterion. Loom trials with large responses (dark blue) and small responses (light blue). No-loom trials with large responses (dark orange) and small responses (light orange).

See also Videos S1 and S2.

saccades.[6,7] The fact that we observed the same *Vm* and L–R WBA correlation in the loom window, in which the fly showed variable behavioral responses, suggests that similar motor-related input arrives to HS during spontaneous and loom-evoked turns. The observed correlation could, in principle, also have occurred from this fly performing spontaneous saccades around the time of the visual expansion while completely ignoring the loom. However, the large changes in the average L–R WBA traces, indicating leftward turns, around the time of the real loom compared to the no-loom (compare dark L–R WBA traces in the right column of Figures 2E and 2H) argue that the fly performed bona fide visually evoked turns away from the expanding disc.

Do the arguments laid out for the single cell and fly in Figure 2 hold for our entire population? Across all our recorded neurons (n = 9), we observed a significant linear relationship between behavioral and neuronal responses during loom trials (Figure 3A, blue dots, r = 0.8, slope = 0.19 mV/deg) and during no-loom trials (Figure 3A, red dots, r = 0.6, slope = 0.19 mV/deg). Importantly, the distributions of ΔL–R WBA clearly differed between these two conditions: in the no-loom condition the mean behavioral response was slightly positive (indicating a weak rightward turn) (mean ΔL–R WBA = 1.7 deg), whereas during the loom condition the mean behavioral response was strongly negative (indicating a leftward turn, i.e., a turn away from the looming stimulus) (mean ΔL–R WBA = −7.0 deg) (Figure 3A). This result demonstrates that the flies indeed were responding to the looming disc on many trials and thus the similar correlation observed in loom and no-loom trials supports the hypothesis that a consistent motor-related signal arrives to HS cells during both spontaneous and loom-evoked turns.

To visualize the presumed motor-related input to HS cells as a function of time, we plotted the mean *Vm* from trials with large and small behavioral responses separately (Figure 3B, selected based on the difference between the mean L-R WBA in the 120-ms baseline and response time windows described earlier) (STAR Methods). In loom trials, a large average behavioral

response was associated with a large average *Vm* hyperpolarization (Figure 3B, dark blue), and a small average behavioral response (Figure 3B, light blue) was associated with a small *Vm* hyperpolarization, as expected (Figure 3B, blue arrowheads). Small-response trials were associated with low pre-stimulus *Vm* and L–R WBA—i.e., a nystagmus saccade prior to the loom—emphasizing again that some of the behavioral-neuronal correlation in Figure 3A was due to nystagmus saccades causing a fluctuating baseline.

To test whether loom-associated modulations of HS cells are correlated with behavior independently of nystagmus saccades, we had sufficient recorded trials across our population to analyze only trials in which the animals did not make a nystagmus saccade prior to the loom. Trials with a high baseline *Vm*, indicating no SRP prior to the loom (STAR Methods), showed a similar, significant, linear relationship between behavioral and neuronal responses during loom trials ($r = 0.8$, slope = 0.17 mV/deg) and no-loom trials ($r = 0.5$, slope = 0.14 mV/deg) (Figure 3C). In these no-nystagmus trials, we observed a seemingly bimodal ΔL–R WBA distribution (Figure 3C, blue distribution at top), which would suggest that flies either responded or did not respond to the loom on any given trial. A statistical test for bimodality, however, did not achieve significance ($p > 0.05$, UniDip) (STAR Methods).[20] A statistically significant bimodality was, however, evident in the distribution of *Vm* changes across trials (Figure 3C, blue distribution at right, 0.025 significance level, UniDip). Average time-domain traces (Figure 3D) emphasize that the correlation between behavioral and neuronal responses are evident even in the context of stable L–R WBA and *Vm* baselines (Figure 3D, blue traces). Overall, these data argue that HS cells receive motor-related inputs during loom-evoked turns, not just spontaneous ones.

Note that the strong correlation between behavior and neuronal responses in Figure 3 does not necessarily mean that SRP magnitude scales with L–R WBA magnitude on each saccade. Rather, once a tethered-flight saccade is executed, HS cells might express an SRP with a relatively consistent size, irrespective of the size of the L–R WBA deflection (see, for example, Figure 2B). In this view, on any given trial, flies either saccade away from the loom or do not, and HS cells get a consistent motor-related input on saccade trials. In other words, there are two sets of blue points in Figure 3C, one set related to responder trials (in the bottom left) and another related to non-responder trials (in the middle), with a strong correlation arising only when both sets are taken into account. Even if this interpretation is correct and our measured L–R WBA saccades in tethered flight are associated with a nominally consistent SRP, it does not rule out the possibility that SRPs in free flight are in fact tuned in strength to the expected visual input on a turn-by-turn basis. Future work will be needed to fully resolve this issue.

The loom-evoked modulation is consistent with a strong motor-related input interacting linearly with a weaker visual input

We observed a consistent, brief deflection in the population's *Vm* on trials with weak behavioral responses (Figures 3B and 3D, black arrows). A similar potential was evident in the single-cell example shown earlier (Figure 2E, blue arrow). Perhaps this signal reflects a small, looming-disc-associated visual input to HS cells, present on all trials independent of behavior? We favor this interpretation because when we recorded *Vm* responses to the same stimulus in non-flying, quiescent flies, we observed a very similar *Vm* signal as in the weak responder trials during flight (Figure 4A, yellow curve). In non-flight, it is reasonable to imagine that the observed *Vm* modulations to a looming stimulus largely reflect a feedforward visual input because the fly was not producing an overt locomotor turn. The *Vm* signal we measured during large-response flight trials would be, in this interpretation, the result of the feedforward visual drive combined with a motor-related input. Under the assumption that visual and motor-related inputs sum linearly—an assumption that is not unreasonable in these non-spiking neurons[7]—one could estimate the shape of the average motor-related signal during loom-evoked saccades by subtracting the signal during small-response trials (the putative visual component) from the signal measured during large-response trials (the putative visual component summed with a motor-related component) (Figure 4A, dark and light gray). This subtracted "L–S" curve (Figure 4B, black) resembles a spontaneous-saccade SRP (Figure 4B, red trace), consistent with the hypothesis that the *Vm* trace in flight reflects the sum of motor and visual inputs to these cells.

The timing of SRPs argues that the motor-related inputs aim to counteract head-movement-related visual input

While the SRPs associated with spontaneous turns (red) and the proposed SRPs for loom-evoked turns (black) in Figure 4B had a similar overall shape, the onset time of the initial dip differed between the two curves. We quantified this onset-timing difference by calculating the moment at which each signal reached 30% of its peak deviation (STAR Methods). The measured, spontaneous saccade SRP (Figure 4B, top, red trace) started dipping ~40 ms earlier relative to the onset of the turn—as measured in the wings' L–R WBA trace—by comparison to the inferred loom-associated SRP (Figure 4B, top, black trace), which seemed to dip closer to turn onset. One concern is that the black trace in Figure 4B is rather derived (a subtraction of two population-averaged *Vm* curves), which might induce a variety of artifacts. If we instead, more simply, extract saccades in the post-loom time window (which should enrich for loom-evoked saccades over spontaneous ones) and compare their associated SRPs to those observed in association with saccades made in the pre-loom time window (spontaneous saccades), we also observed a trend for the SRP to start earlier relative to the L–R WBA saccades on spontaneous turns, in this case by ~20 ms (Figures 4C and 4D). In loom-evoked turns we thus observed that SRPs start to become evident at roughly the same time as the L–R WBA saccade signal (Figure 4D), arguing against the notion that SRPs in HS cells drive the loom-evoked saccades to take place.

How might one explain the timing differences between spontaneous and loom-evoked SRPs? Past work has revealed that when HS cells are silenced, head movements made to stabilize the visual image are smaller in magnitude and made more slowly than normal; L–R WBA wing steering signals are only mildly impaired (if impaired at all).[7] We therefore measured the timing of head, wing, and abdomen movements made in association with spontaneous and loom-evoked saccades (Figures 4E–4J). We tethered the fly's thorax to a rigid pin with the head

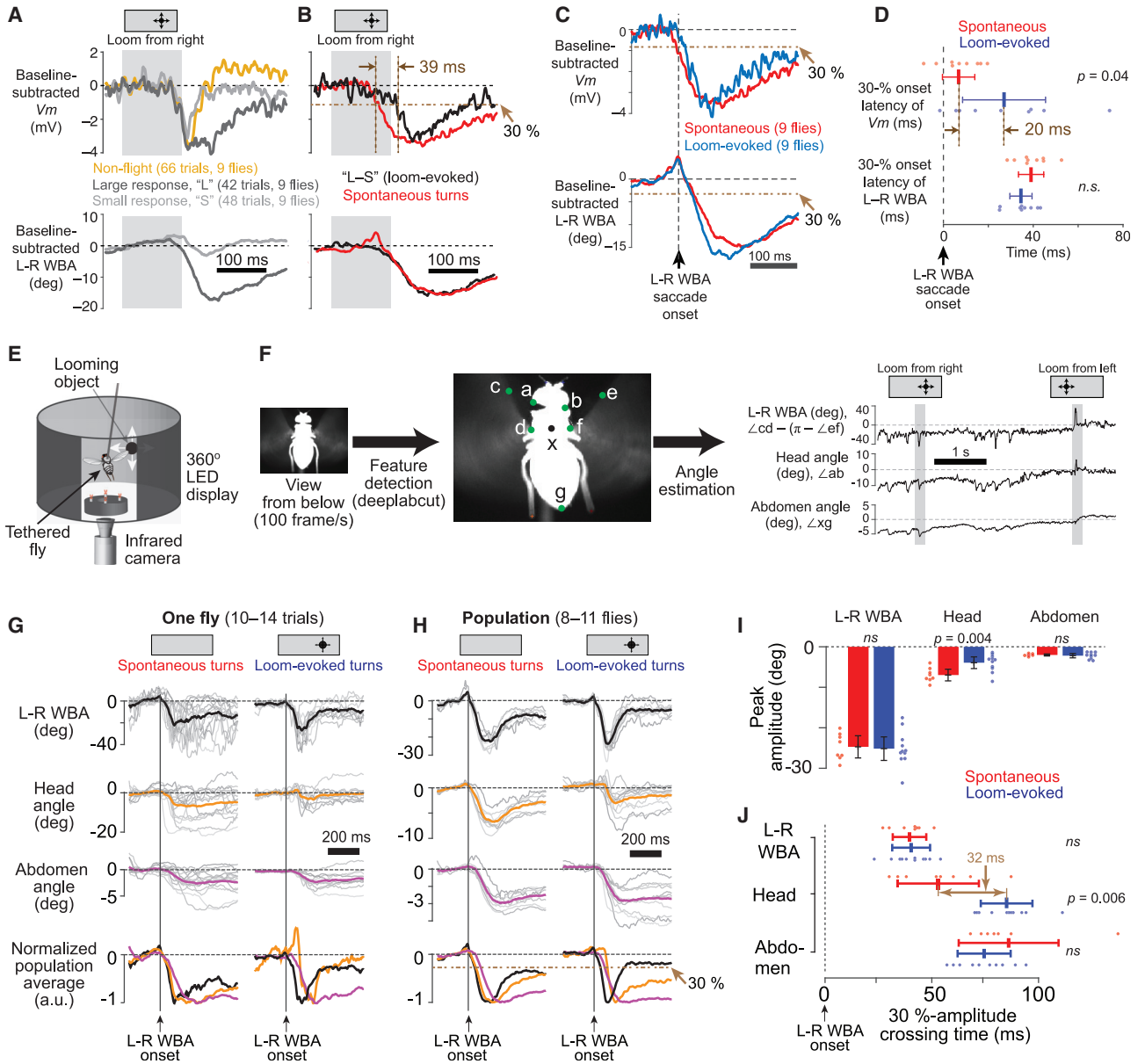

Figure 4. Motor-related inputs to HS cells as well as the onset of head movements are delayed relative to the wing-steering response on loom-evoked turns

(A) Population-averaged L–R WBA and *Vm* from large-response (dark gray) and small-response (light gray) no-nystagmus-saccade loom trials. Mean *Vm* in response to the loom stimulus from non-flying flies is also shown (yellow).

(B) Population-averaged L–R WBA and *Vm* from nystagmus/spontaneous saccades (red). The time-point-by-time-point subtraction of the dark gray and gray traces on the right is shown in black here (black, "L-S").

(C) Population-averaged saccade-triggered L–R WBA and *Vm* for loom-evoked (blue) and spontaneous saccades (red).

(D) The time at which L–R WBA and *Vm* reach 30% of their peak deviation. Each point represents one fly. Error bars indicate 95% confidence intervals.

(E) A schematic of the experimental setup for pin-tethered flight.

(F) A DeepLabCut neural network computes the L–R WBA, head-to-thorax, and abdomen angles at 100 Hz.

(G) Saccade-triggered averages of L–R WBA, head angle, and abdomen angle for a sample fly (thin lines, single trials; thick lines, mean).

(H) Same as (E), but population averaged traces (thin lines, single fly averages; thick line, mean).

(I) Peak angular amplitude of the L–R WBA, head, and abdomen signals during spontaneous and loom-evoked saccades (dots, single fly means). Error bars indicate 95% confidence intervals.

(J) The time at which L–R WBA, head, and abdomen angles reach 30% of their peak deviation after saccade onset.

See also Figure S1.

unglued,[21,22] and we used a deep neural network[23] to track the position of body parts, imaged at 100 Hz, during tethered-flight saccades (Figures 4E–4J). Head movements associated with saccades were generally delayed in relation to L–R WBA wing-steering movements (Figure 4J),[6] but the delay was 32 ms shorter (and more variable) for spontaneous saccades in comparison to loom-evoked saccades (Figure 4J). This timing relationship remained unchanged when we selected saccades with a different method (STAR Methods) (Figure S1). The 32-ms timing difference in the onset time of head movements is similar to the 20–40 ms timing difference between spontaneous and loom-evoked SRPs in our electrophysiology experiments (Figures 4A and 4B), supporting the hypothesis that SRPs reflect motor-related inputs that aim to suppress the visual activation associated with head movements during saccades. In other words, when head movements occur earlier on a given saccade, SRPs arrive earlier to HS cells as well.

Optomotor responses are not associated with measurable motor-related inputs to optic-flow processing neurons

If both spontaneous and loom-evoked saccades are associated with motor-related inputs to HS cells, perhaps all flight turns are associated with such inputs? An observation that gave us pause with regard to this idea was that when the widefield grating in our electrophysiological experiments first started to rotate—well before the loom—and the HS cells' *Vm* thus rapidly depolarized, we did not observe a strong correlation between the *Vm* of HS cells and L–R WBA (r = 0.2 in Figures 5A and 5B versus r = 0.5–0.8 in Figures 3A and 3C). Flies presented with widefield, rotational visual motion perform a so-called optomotor response, i.e., a turn in the same direction as the panoramic motion. The low correlation in Figure 5B thus suggested that motor-related inputs may not arrive to HS cells during optomotor responses. An important concern, however, was that the rise in the L–R WBA curve in Figure 5A was very slow by comparison to the rapidly changing L–R WBA signals during saccades. Furthermore, HS cells were depolarized close to saturation in these experiments, and putative motor-related signals for optomotor turns would have been expected to have the same sign as the strong visual responses. To properly test whether motor-related inputs arrive to HS cells during optomotor responses, we sought to elicit fast optomotor turns that mimicked, as closely as possible, the turning dynamics during spontaneous and loom-evoked saccades, while using visual stimuli that induced as little a visual response as possible.

We again tonically depolarized the HS cells, but this time by presenting a panoramic starfield, rather than a square-wave grating, which rotated in the preferred direction of the cells on all trials. That is, the starfield rotated clockwise because we recorded from HS cells on the right side (Figures 5C and 5D). On optomotor trials, we presented an irregularly spaced, vertical grating overlayed on the starfield on the contralateral side. This grating rapidly rotated counterclockwise by 11.25° in 120 ms (Figure 5C; Video S3), inducing a fast, leftward optomotor response. We used a grating with irregularly spaced stripes[6] because gratings with regularly spaced stripes induce an unnatural, oscillatory *Vm* response in HS cells when moved extremely fast (data not shown). On loom trials, we presented a looming disc over the starfield on the ipsilateral side (Figure 5D; Video S4), inducing a loom-evoked, leftward saccade, akin to those elicited in the experiments described in Figures 2 and 3.

Flies responded with rapid, leftward turns both to the optomotor grating and to the looming disc (Figure 5E). The *Vm* changes made in association with the looming disc were generally larger than those observed in response to the grating. Like in our initial dataset, the *Vm* change to the looming disc in flying flies (Figures 5E and 5F, top, green and blue traces) exceeded the response to the same stimulus measured in non-flying, quiescent flies (Figures 5E and 5F, top, magenta traces); the difference between the blue and magenta curves in Figures 5E and 5F reflects, in our interpretation, a motor-related input to HS cells during loom-evoked saccades. The size of the loom-evoked SRP in this dataset (Figure 5F, right, difference between magenta and blue traces in loom trials) was smaller than that observed in the first dataset (Figures 2 and 3), likely because the starfield did not depolarize the HS cell from rest as much as the square-wave grating did, and the less depolarized an HS cell is at the time of a saccade, the smaller the measured SRP.[6,7]

Unlike with loom trials, in optomotor trials, the small *Vm* deflection observed during the visual stimulus was nearly identical in flying and non-flying flies (Figure 5F, compare green and magenta curves on the left and bar plots on the right), arguing that HS cells receive only a very weak or no motor-related modulation during optomotor flight turns. The lack of an obvious SRP is all the more notable given that flies are likely attempting to perform very large, gaze-stabilizing head movements in response to the fast optomotor stimulus based on behavioral analyses of pin-tethered flies whose heads were free as they viewed a very similar optomotor stimulus (Figure S2; Video S5).

One concern is that the flies' optomotor responses in the above experiments, while fast, still did not reach the peak L–R WBA velocities observed during loom saccades (compare the peak slopes of blue and green traces in Figure 5F, bottom). Perhaps SRPs are only evident during extremely fast L–R WBA changes? We therefore selected for the 20 loom saccade trials (across all flies) with the smallest L–R WBA onset slope and the 20 optomotor trials (across all flies) with the largest L–R WBA onset slope, to equalize the measurable kinematics in our preparation (STAR Methods). In these trials, the average speed at which the wings performed an optomotor turn was even faster than that of the correspondingly analyzed loom-evoked saccades, yet the loom-evoked saccades still arrived with an apparent SRP and the optomotor responses did not (Figure 5G).

DISCUSSION

We discovered that loom-evoked flight turns are associated with suppressive, motor-related inputs to HS cells (Figures 2 and 3), similar to those previously reported during spontaneous flight turns.[6,7] The timing of motor-related inputs to HS cells argues that these neurons, at least in part, function to regulate gaze-stabilizing head movements (Figure 4) and that their motor-related inputs aim to briefly suppress this gaze-stabilizing function during intended course-changing turns. Motor-related inputs were not detectable in HS cells during optomotor or course-stabilizing turns (Figure 5). Overall, these findings argue that a given action

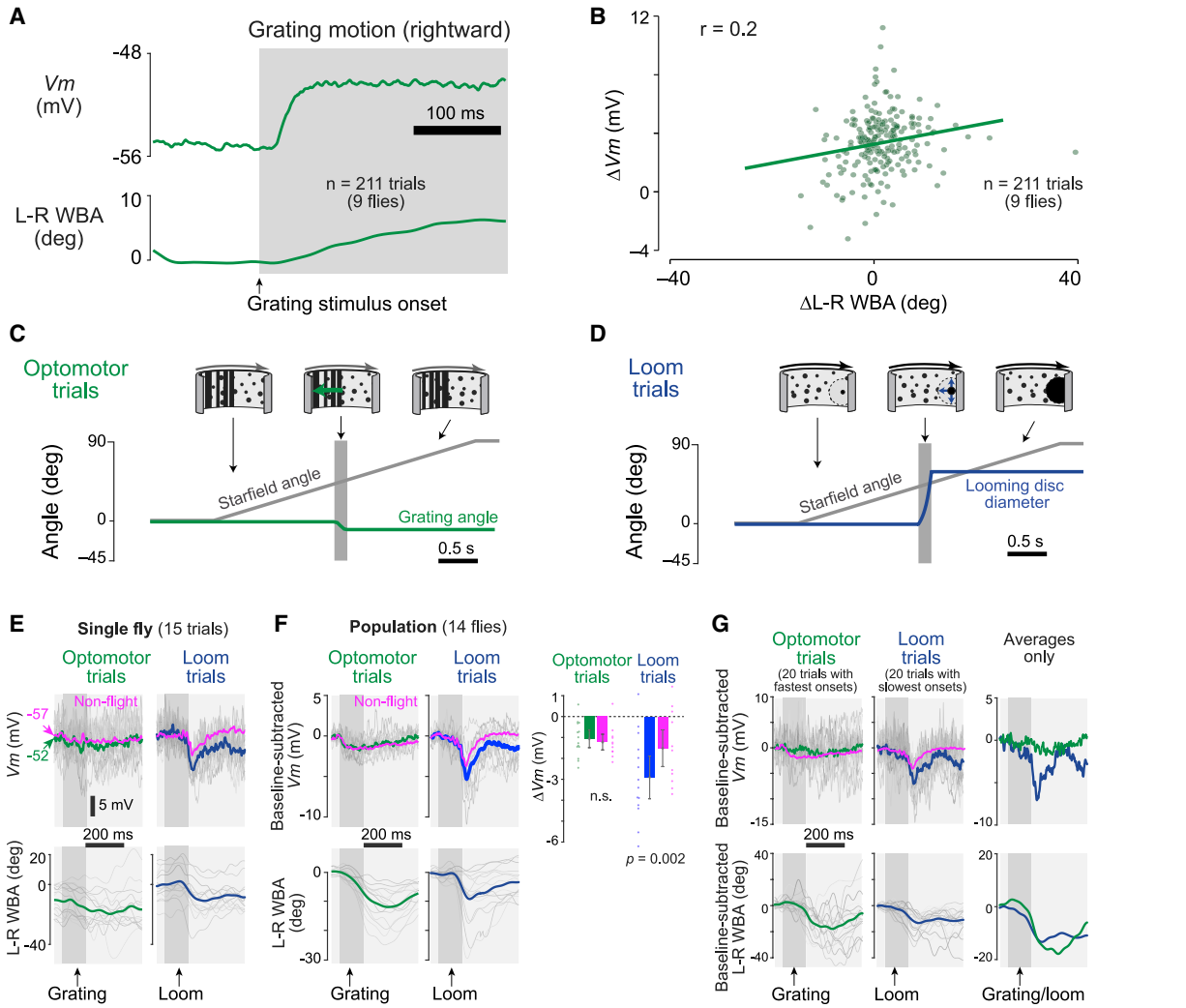

Figure 5. Optomotor turns are not associated with detectable motor-related inputs to HS cells

(A) Population-averaged L–R WBA and *Vm* at the onset of grating motion from the experiments of Figures 2 and 3.

(B) Δ*Vm* versus ΔL-RWBA at the onset of grating motion in loom trials. To generate the ΔL–R WBA and Δ*Vm* signals plotted, we subtracted the L–R WBA and *Vm* signals in 120-ms windows before and after grating-motion onset (211 trials from 9 flies). Linear fit (r = 0.2, slope = 0.07, p = 0.005).

(C) Rotating starfield pattern with an overlayed fast, leftward-sweeping, irregularly spaced, vertical grating on the left (Video S3).

(D) Rotating starfield pattern with an overlayed looming disc from the right (Video S4).

(E) L–R WBA and *Vm* from a single fly, on optomotor trials (left) and loom trials (right). Responses from the same cell in non-flight are shown in magenta (thin lines, single trials; thick line, mean). The commonly observed ~5 mV flight-induced baseline-*Vm* offset[6] has been nulled between the two traces.

(F) Same as (E) but the population averages (left) (thin lines, single fly averages; thick line, mean). Mean *Vm* changes (Δ*Vm*) were measured as the amplitude difference between the 120 ms following the visual motion (loom or grating) and 120 ms preceding the motion (right, paired t test). Error bars indicate the 95% confidence intervals.

(G) L–R WBA and *Vm* from 20 optomotor trials (out of 179 trials from 14 flies) with the fastest onset slope and 20 loom trials (out of 180 trials from 14 flies) with the slowest onset slope were selected so that the L–R WBA signals had similar maximum slopes in the loom and optomotor conditions. Rightmost column shows the same data from the left and middle column, but overlayed. Magenta traces are from non-flight, as in (F).

See also Figure S2.

can be variably associated with motor-related feedback signals to the visual system, contingent on the behavioral purpose of the action alongside the function of the visual neuron being modulated.

In mammals, recent work has argued that motor-related activity is widespread across many brain regions, including primary-sensory cortical areas, in the context of diverse behaviors, like whisking, pupil dilation, and locomotion.[3,24–26] In these studies, neural signals were correlated to varied spontaneous and task-related actions. An interesting synergy between vertebrates and invertebrates is that motor-related signals also appear widespread in the insect visual system during spontaneous locomotion.[1,6,7,27–30]

Here we show that motor-related modulations are also evident in HS cells during certain visually evoked turns. HS cell activity is believed to induce corrective head and/or body movements after

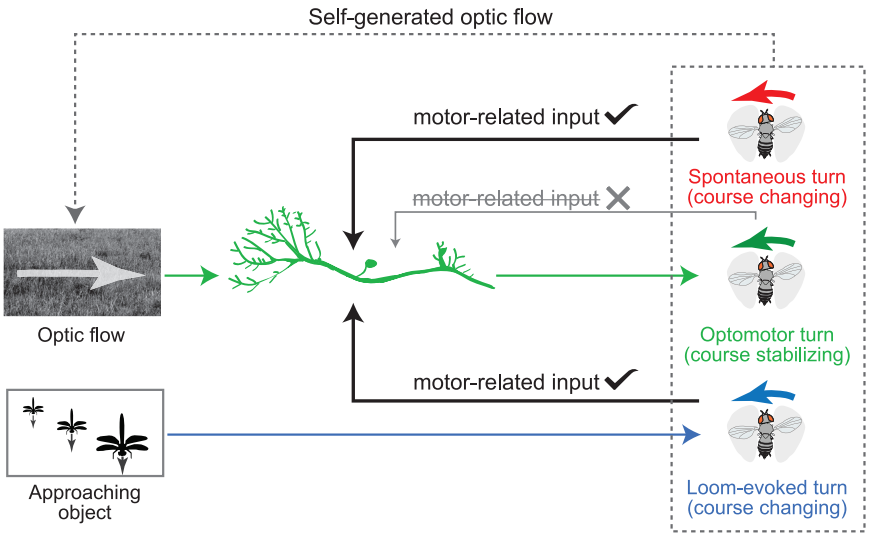

Figure 6. Summary schematic

The fact that we show two efference copy (motor-related input) pathways is not meant to imply that two different neurons or neuron populations necessarily bring this signal to the visual system in these two contexts.

unintended deviations to the fly's locomotor course or head gaze angle,[7,22,31–34] thus helping to maintain flight- or gaze-angle stability. In this light, it makes sense that the visual activation of HS cells should be silenced via motor-related inputs during loom-evoked turns because these turns aim to purposefully change the fly's flight or gaze angle. Optomotor responses, on the other hand, are turns that aim to fix an unintended deviation in the course/gaze angle, and it seems sensible that HS cell activity would not be modulated for these turns because their activity exists exactly to guide these turns.

In 1980, Tom Collett analyzed the trajectories of hoverflies freely flying in the context of a rotating striped drum—which induces slow optomotor turns—while concurrently performing object-orienting (tracking) turns related to the act of chasing a conspecific.[15] His elegant analyses suggested the possibility of optomotor responses being suppressed during object-orienting turns via efference copies. However, with only behavioral measurements he could not differentiate this hypothesis from other hypotheses that did not involve efference copies. Here, we provide physiological evidence for the view that optomotor responses are indeed actively suppressed (at the level of HS cells, if not earlier) during object-orienting (in our case, loom-evoked) turns. Thus, our results open the door to a more detailed, cellular, and circuit-level understanding of how parallel visuomotor reflexes interact to yield a coherent, singular, behavioral stream during natural behavior—a fundamental issue in animal behavior and autonomous robotics.[15,35,36]

Like in flies, motor-related feedback signals to the primate gaze-control system have been inferred to exist or directly measured,[37,38] and these motor-related modulations are thought to accompany all "voluntary" and some "involuntary" eye movements.[39] Human psychophysical experiments have revealed that voluntary saccades as well as reactive saccades are associated with so-called saccadic suppression, albeit with slightly different strengths of suppression for different types of saccades.[40] The slow phase of the optokinetic reflex, however, is hypothesized to not be accompanied by efference copy signals .[39] Both of these ideas are supported by our electrophysiological data in flies; we find suppressive inputs during spontaneous as well as loom-evoked, reactive saccades, but only small or absent modulations during optomotor turns (Figure 6), which stabilize gaze like the slow phase of the optokinetic reflex in humans. In both flies and humans, it thus seems that many aspects of visual processing are left unmodulated during eye movements made for the purpose of stabilizing gaze, while purposeful gaze changes are accompanied by clear motor-related modulations.[41,42]

STAR★METHODS

Detailed methods are provided in the online version of this paper and include the following:

- KEY RESOURCES TABLE
- RESOURCE AVAILABILITY
  - Lead contact
  - Materials availability
  - Data and code availability
- EXPERIMENTAL MODEL AND SUBJECT DETAILS
  - Fly Stocks
- METHOD DETAILS
  - Visual displays
  - Visual Stimuli
  - Behavioral Electrophysiology
  - Purely Behavioral Experiments
- QUANTIFICATION AND STATISTICAL ANALYSIS
  - Data analysis
  - Statistical analysis

SUPPLEMENTAL INFORMATION

Supplemental information can be found online at https://doi.org/10.1016/j.cub.2021.09.068.

ACKNOWLEDGMENTS

We thank all members of the Maimon lab for helpful discussions. We acknowledge a Leon Levy Fellowship in Mind, Brain and Behavior and postdoctoral Kavli Fellowship to L.M.F. G.M. is a Howard Hughes Medical

Institute Investigator. A.J.K. acknowledges National Research Foundation of Korea (NRF) grants funded by the Korea Government (MSIT) NRF-2020R1A4A1016840 and NRF-2021M3E5D2A01023888.

AUTHOR CONTRIBUTIONS

All three authors designed the experiments. L.M.F. and A.J.K. collected and analyzed the electrophysiological data with input from G.M. A.J.K. collected and analyzed the behavioral data with input from G.M. and L.M.F. All three authors contributed to the writing of the paper.

DECLARATION OF INTERESTS

The authors declare no competing interests.

Received: July 19, 2021
Revised: September 10, 2021
Accepted: September 23, 2021
Published: October 12, 2021

REFERENCES

1. Maimon, G., Straw, A.D., and Dickinson, M.H. (2010). Active flight increases the gain of visual motion processing in *Drosophila*. Nat. Neurosci. *13*, 393–399.
2. Saleem, A.B., Ayaz, A., Jeffery, K.J., Harris, K.D., and Carandini, M. (2013). Integration of visual motion and locomotion in mouse visual cortex. Nat. Neurosci. *16*, 1864–1869.
3. Stringer, C., Pachitariu, M., Steinmetz, N., Reddy, C.B., Carandini, M., and Harris, K.D. (2019). Spontaneous behaviors drive multidimensional, brainwide activity. Science *364*, 255.
4. Niell, C.M., and Stryker, M.P. (2010). Modulation of visual responses by behavioral state in mouse visual cortex. Neuron *65*, 472–479.
5. Keller, G.B., Bonhoeffer, T., and Hübener, M. (2012). Sensorimotor mismatch signals in primary visual cortex of the behaving mouse. Neuron *74*, 809–815.
6. Kim, A.J., Fitzgerald, J.K., and Maimon, G. (2015). Cellular evidence for efference copy in *Drosophila* visuomotor processing. Nat. Neurosci. *18*, 1247–1255.
7. Kim, A.J., Fenk, L.M., Lyu, C., and Maimon, G. (2017). Quantitative predictions orchestrate visual signaling in *Drosophila*. Cell *168*, 280–294.e12.
8. Censi, A., Straw, A.D., Sayaman, R.W., Murray, R.M., and Dickinson, M.H. (2013). Discriminating external and internal causes for heading changes in freely flying *Drosophila*. PLoS Comput. Biol. *9*, e1002891.
9. Heisenberg, M., and Wolf, R. (1979). On the fine structure of yaw torque in visual flight orientation of *Drosophila melanogaster*. J. Comp. Physiol. *130*, 113–130.
10. Lindsay, T., Sustar, A., and Dickinson, M. (2017). The function and organization of the motor system controlling flight maneuvers in flies. Curr. Biol. *27*, 345–358.
11. Maye, A., Hsieh, C.H., Sugihara, G., and Brembs, B. (2007). Order in spontaneous behavior. PLoS ONE *2*, e443.
12. Muijres, F.T., Elzinga, M.J., Melis, J.M., and Dickinson, M.H. (2014). Flies evade looming targets by executing rapid visually directed banked turns. Science *344*, 172–177.
13. Tammero, L.F., and Dickinson, M.H. (2002). Collision-avoidance and landing responses are mediated by separate pathways in the fruit fly, *Drosophila melanogaster*. J. Exp. Biol. *205*, 2785–2798.
14. von Holst, E., and Mittelstaedt, H. (1950). The principle of reafference: interactions between the central nervous system and the peripheral organs. Naturwissenschaften *37*, 464–476.
15. Collett, T.S. (1980). Angular tracking and the optomotor response an analysis of visual reflex interaction in a hoverfly. J. Comp. Physiol. *140*, 145–158.
16. Hausen, K. (1982). Motion sensitive interneurons in the optomotor system of the fly II: the horizontal cells: receptive field organization and response characteristics. Biol. Cybern. *46*, 67–79.
17. Schnell, B., Joesch, M., Forstner, F., Raghu, S.V., Otsuna, H., Ito, K., Borst, A., and Reiff, D.F. (2010). Processing of horizontal optic flow in three visual interneurons of the *Drosophila* brain. J. Neurophysiol. *103*, 1646–1657.
18. Honrubia, V., Downey, W.L., Mitchell, D.P., and Ward, P.H. (1968). Experimental studies on optokinetic nystagmus. II. Normal humans. Acta Otolaryngol. *65*, 441–448.
19. Gabbiani, F., Krapp, H.G., and Laurent, G. (1999). Computation of object approach by a wide-field, motion-sensitive neuron. J. Neurosci. *19*, 1122–1141.
20. Maurus, S., and Plant, C. (2016). Skinny-dip: clustering in a sea of noise. Proceedings of the 22nd ACM SIGKDD International Conference on Knowledge Discovery and Data Mining, 1055–1064.
21. Maimon, G., Straw, A.D., and Dickinson, M.H. (2008). A simple vision-based algorithm for decision making in flying *Drosophila*. Curr. Biol. *18*, 464–470.
22. Cellini, B., and Mongeau, J.M. (2020). Active vision shapes and coordinates flight motor responses in flies. Proc. Natl. Acad. Sci. USA *117*, 23085–23095.
23. Mathis, A., Mamidanna, P., Cury, K.M., Abe, T., Murthy, V.N., Mathis, M.W., and Bethge, M. (2018). DeepLabCut: markerless pose estimation of user-defined body parts with deep learning. Nat. Neurosci. *21*, 1281–1289.
24. Shusterman, R., Smear, M.C., Koulakov, A.A., and Rinberg, D. (2011). Precise olfactory responses tile the sniff cycle. Nat. Neurosci. *14*, 1039–1044.
25. Musall, S., Kaufman, M.T., Juavinett, A.L., Gluf, S., and Churchland, A.K. (2019). Single-trial neural dynamics are dominated by richly varied movements. Nat. Neurosci. *22*, 1677–1686.
26. Schneider, D.M., Sundararajan, J., and Mooney, R. (2018). A cortical filter that learns to suppress the acoustic consequences of movement. Nature *561*, 391–395.
27. Seelig, J.D., Chiappe, M.E., Lott, G.K., Dutta, A., Osborne, J.E., Reiser, M.B., and Jayaraman, V. (2010). Two-photon calcium imaging from head-fixed *Drosophila* during optomotor walking behavior. Nat. Methods *7*, 535–540.
28. Tuthill, J.C., Nern, A., Rubin, G.M., and Reiser, M.B. (2014). Wide-field feedback neurons dynamically tune early visual processing. Neuron *82*, 887–895.
29. Fujiwara, T., Cruz, T.L., Bohnslav, J.P., and Chiappe, M.E. (2017). A faithful internal representation of walking movements in the *Drosophila* visual system. Nat. Neurosci. *20*, 72–81.
30. Strother, J.A., Wu, S.-T., Rogers, E.M., Eliason, J.L.M., Wong, A.M., Nern, A., and Reiser, M.B. (2018). Behavioral state modulates the ON visual motion pathway of *Drosophila*. Proc. Natl. Acad. Sci. USA *115*, E102–E111.
31. Dvorak, D.R., Bishop, L.G., and Eckert, H.E. (1975). On the identification of movement detectors in the fly optic lobe. J. Comp. Physiol. *100*, 5–23.
32. Geiger, G., and Nässel, D.R. (1981). Visual orientation behaviour of flies after selective laser beam ablation of interneurones. Nature *293*, 398–399.
33. Hausen, K., and Wehrhahn, C. (1983). Microsurgical lesion of horizontal cells changes optomotor yaw responses in the blowfly *Calliphora erythrocephala*. Proc. Royal Soc. Lond. Ser. B. Biological Sci. *219*, 211–216.
34. Haikala, V., Joesch, M., Borst, A., and Mauss, A.S. (2013). Optogenetic control of fly optomotor responses. J. Neurosci. *33*, 13927–13934.
35. Webb, B. (2002). Robots in invertebrate neuroscience. Nature *417*, 359–363.
36. Webb, B.H., and Harrison, R.R. (2000). Integrating sensorimotor systems in a robot model of cricket behavior. Proc. SPIE *4196*, 113–124.

37. Bridgeman, B., Hendry, D., and Stark, L. (1975). Failure to detect displacement of the visual world during saccadic eye movements. Vision Res. *15*, 719–722.

38. Cavanaugh, J., Berman, R.A., Joiner, W.M., and Wurtz, R.H. (2016). Saccadic corollary discharge underlies stable visual perception. J. Neurosci. *36*, 31–42.

39. Bridgeman, B. (1995). A review of the role of efference copy in sensory and oculomotor control systems. Ann. Biomed. Eng. *23*, 409–422.

40. Gremmler, S., and Lappe, M. (2017). Saccadic suppression during voluntary versus reactive saccades. J. Vis. *17*, 8.

41. Crapse, T.B., and Sommer, M.A. (2008). Corollary discharge across the animal kingdom. Nat. Rev. Neurosci. *9*, 587–600.

42. Sommer, M.A., and Wurtz, R.H. (2008). Brain circuits for the internal monitoring of movements. Annu. Rev. Neurosci. *31*, 317–338.

43. Reiser, M.B., and Dickinson, M.H. (2008). A modular display system for insect behavioral neuroscience. J. Neurosci. Methods *167*, 127–139.

STAR★METHODS

KEY RESOURCES TABLE

REAGENT or RESOURCE	SOURCE	IDENTIFIER
Deposited data		
Electrophysiogical and behavioral data	This paper	https://doi.org/10.6084/m9.figshare.15169602
Experimental models: Organisms/strains		
Drosophila: w^{1118};+;R81G07-GAL4	Bloomington Drosophila Stock Center	Stk#40122
Drosophila: Wild-type Canton S	Martin Heisenberg	N/A
Drosophila: w^{1118}/+;UAS-2xEGFP/+;R81G07-GAL4/+	[7]	N/A
Software and algorithms		
MATLAB	MathWorks	http://www.mathworks.com
Real-time wingbeat analysis for tethered, flying flies	Andrew Straw	https://github.com/motmot/strokelitude
Post hoc head angle analysis for tethered flies	this paper	N/A
DeepLabCut	[23]	https://github.com/DeepLabCut/DeepLabCut
UniDip	[20]	https://github.com/BenjaminDoran/unidip
WinEDR	University of Strathclyde, Glasgow	https://spider.science.strath.ac.uk/sipbs/software_ses.htm
AxoScope, pClamp 10	Molecular Devices	https://www.moleculardevices.com/

RESOURCE AVAILABILITY

Lead contact

Further information and requests for reagents should be directed to and will be fulfilled by the Lead Contact, Gaby Maimon (maimon@rockefeller.edu).

Materials availability

This study did not generate new unique reagents. Requests of fly stocks should be directed to and will be fulfilled by the Lead Contact, Gaby Maimon (maimon@rockefeller.edu).

Data and code availability

All stimulus pattern files as well as behavioral and electrophysiological data can be accessed at https://doi.org/10.6084/m9.figshare.15169602. Further information and requests for data and code should be directed to and will be fulfilled by the Lead Contact, Gaby Maimon (maimon@rockefeller.edu).

EXPERIMENTAL MODEL AND SUBJECT DETAILS

Fly Stocks

We used female *Drosophila melanogaster* that were 1-2 days post-eclosion for behavioral electrophysiology and 2-5 days post-eclosion for purely behavioral experiments. Flies were reared on standard corn-meal agar, in 25°C incubators with a 12 h light/dark cycle. To visualize HS cells for the whole-cell patch clamping experiment, we used either w^{1118};+;R81G07-GAL4 crossed to +;+;UAS-2XEGFP or w^{1118};UAS-2XEGFP;R81G07-GAL4 crossed to Heisenberg Canton S wild-type flies. Flies were cold-anesthetized and tethered either to a tungsten pin for the purely behavioral experiments or to a custom plate for the electrophysiology experiments.[1]

METHOD DETAILS

Visual displays

We used standard LED displays, described previously.[43] Visual stimuli for purely behavioral experiments (Figures 4E–4J, S1, and S2) were displayed on a cylindrical LED arena with (570 nm) green LEDs covering 360° in azimuth and 94° in elevation. One LED pixel subtended ~3.75°. Visual stimuli for electrophysiological experiments (Figures 1, 2, 3, 4, and 5) were presented on a cylindrical LED arena with (570 nm) green LEDs that subtended 216° in azimuth and 76° in elevation. One LED pixel subtended ~2.25° in

this visual display. The visual display used in electrophysiological experiments was tilted ~65° from vertical, such that the axis of horizontal motion on the display was roughly aligned with the yaw motion-detection axis of the compound eyes.[7]

Visual Stimuli

Loom stimuli, in all experiments, employed a dark expanding disc. The disc size always increased via an arc-tangent function of time to mimic a visual object approaching the fly at a constant speed.

Stimuli for electrophysiology – loom (Figures 2 and 3)

The stimulus presented for the electrophysiological experiments in Figures 2 and 3 combined a moving square-wave grating—which encompassed the entire contralateral hemisphere and extended 54° into the ipsilateral hemisphere—with a looming disc on the ipsilateral side (Video S1). A control stimulus was identical except that the looming disc never expanded (Video S2). The moving grating had an 18° period and moved with a temporal frequency of 1 Hz (i.e., 1 cycle/s). The looming disc expanded over 120 ms, starting 2 s after the onset of grating motion, from an initial diameter of 11.25° to a final diameter of 54°, i.e., with a half-size to approach velocity value of l/[v] ~15 ms. Both the looming disc and the grating had a nominal contrast of 100%, though reflections likely reduced this value.

Stimuli for electrophysiology – loom versus optomotor stimuli (Figure 5)

For the experiments in Figure 5, we expanded a looming disc on the right in the context of a panoramic starfield rotating clockwise (Video S3). On other trials, there was no looming disc on the right, but instead we rapidly moved an irregularly spaced grating, on the left, 11.25° counterclockwise, overlaid on the moving starfield, which was also present (Video S4). The rapid grating motion, and the loom expanded, over a 120-ms time window, beginning 1.5 s after the starfield started moving. To generate the grating overlaid on the starfield,[7] we took the minimum pixel value of the two patterns at each position; taking the minimum simulated a foreground starfield, with dark stars, moving over a grating in the background. To generate the loom overlaid on the starfield, we, more simply, left the region into which the disc would expand brightly lit until the loom happened, which made that region dark (see Video S4). This approach still led the HS cells to be depolarized by the starfield, while also yielding robust turns to the loom.

Stimuli for behavioral experiments (Figures 4, S1, and S2)

In the purely behavioral experiments (Figures 4, S1, and S2), looms were centered 90° to the left or to the right of the tethered, flying fly, with discs that expanded from 7.5° to 52.5° in diameter in 120 ms (l/[v] ~9 ms). For testing optomotor responses (Figure S2; Video S5), we moved a vertically oriented random grating by 33.8 degrees in 120 ms.[6]

Behavioral Electrophysiology

We used standard methods for patch-clamp recordings in tethered, flying flies.[1] In brief, we used blue-light (410 nm) curable glue (Bondic) to attach flies to plastic plates and to immobilize the proboscis. We then removed the cuticle, muscles, and trachea above the brain. We perfused an extracellular solution (275–280 mOSM) that contained in mM: 103 NaCl, 3 KCl, 5 N-Tris(hydroxymethyl) methyl-2-aminoethanesulfonic acid (TES), 10 Trehalose, 10 Glucose, 2 Sucrose, 26 $NaHCO_3$, 1 NaH_2PO_4, 1.5 $CaCl_2$, 4 $MgCl_2$. The solution was bubbled with 95% O_2/5% CO_2 to achieve a pH level of 7.3. Prior to obtaining whole cell recordings, we first desheathed the neurolemma over the HS cells with a 0.5 mg/mL collagenase solution, released from a pipette under manual control, to cleanly expose the plasma membrane of the HS cells. Recording pipettes were filled with intracellular solution that contained in mM: 140 K-Aspartate, 1 KCl, 10 HEPES, 1 EGTA, 0.5 Na_3GTP, and 4 MgATP, 0.02 Alexa-568-hydrazide-Na and 13 Biocytin hydrazide. The membrane voltage was amplified (A-M Systems Model 2400), digitized at 10 kHz (PCIe-6351, National Instruments; Digidata 1440a, Molecular Devices), and saved to a computer (WinEDR, University of Strathclyde; AxoScope, pClamp 10, Molecular Devices). Voltage measurements have been corrected for a 13-mV junction potential. We sometimes injected a small amount of hyperpolarizing current into neurons to neutralize the depolarizing effects of the seal conductance.

During these experiments, videos of flies were taken at 100 Hz from below with an externally triggered infrared-sensitive camera (AVT-GE680), and the wing beat signals were extracted as described previously.[1,6,7]

The GAL4 line used (R81G07-GAL4) labels all six HS cells, three on each side of the brain. We targeted the horizontal system north (HSN) cells but cannot exclude the possibility that we occasionally recorded from horizontal system equatorial cell (HSE) instead of HSN. Both cell types receive comparable motor-related signals[7] and thus none of our central conclusions should be altered by this issue.

Purely Behavioral Experiments

We cold-anesthetized flies and used a blue-light (410 nm) curable glue (Bondic) to attach them to a tungsten pin at the tip of the thorax. The head was not glued to the pin and left free to move. Flies were positioned at the center of a cylindrical LED display and presented with looming and optomotor (rotating grating) visual patterns, presented in pseudorandom order. We took video images of the flying flies from below using the same imaging approach as in the electrophysiological experiments. We analyzed these images, post hoc, using DeepLabCut.[23]

QUANTIFICATION AND STATISTICAL ANALYSIS

Data analysis

For the behavioral-electrophysiology experiments with loom-evoked saccades (Figures 2 and 3), we only analyzed recordings in which flies initiated prolonged flight bouts. Specifically, we excluded three flies for which we could not present enough repetitions of the stimuli during flight and two flies that did not clearly perform any saccades in response to the loom stimulus (suggesting

that we may have damaged the visual system during the dissection). All analyses were done using Python and MATLAB (Mathworks) for Figures 2 and 3. The left-minus-right wingbeat amplitude (L–R WBA) signals were filtered with an 8th-order, forward-backward lowpass filter (Butterworth, cutoff = 25 Hz). Spontaneous saccades (Figures 2E, 2H, 4B, and 4C) were detected by the same algorithm used previously.[6,7] Loom responses are aligned to stimulus onset. Large and small response trials shown in Figures 2E and 2H (single fly data) were chosen based on the difference in the mean L–R WBA in two time windows. The first window encompassed the 120-ms during which the loom took place. The second window encompassed the 120 ms immediately thereafter, after the disc had fully expanded, when the fly's behavioral responses occurred. We plotted the mean ± SEM of the seven largest and seven smallest responses. The large and small response curves in Figures 3B and 3D (population-level analysis) were also selected based on these L–R WBA amplitude changes, and we set threshold values by hand, so as to best obtain approximately equal numbers of large and small wing responses that yielded well separated wing traces in the loom trials.

We selected no-nystagmus trials in Figures 3C and 3D by choosing trials in which the *Vm* prior to the loom was above a threshold, thus isolating trails in which the loom-evoked SRP was less likely to have been influenced by a preceding SRP. Specifically, we considered the mean *Vm* for each fly over all time points and trials as a threshold value. Trials in which the mean *Vm* in an 80 ms window starting 20 ms before the loom was above threshold were considered no-nystagmus-saccade trials.

To analyze the fly's body kinematics in the purely behavioral experiments of Figure 4, we used DeepLabCut[23] to detect the location of seven points on the body on each image frame (Figure 4F). We trained the DeepLabCut network with 90 randomly chosen frames, which were labeled manually, until the "loss value" reached < 0.0005. The network was trained via computation on a GPU (Nvidia GTX 1070Ti). The resulting kinematic variables were combined in MATLAB (Mathworks) with information on the visual stimuli for subsequent analyses.

For the saccade-triggered analyses in Figures 4G–4I, we ran the saccade detection algorithm described previously.[6,7] We then categorized detected saccades depending on their visual context; e.g., one spontaneous/nystagmus set that occurred in the context of the moving grating, but prior to the loom, and another set of loom-evoked saccades that occurred in the 40-100 ms time-window after the start of the looming stimulus. The average amplitude of L–R WBA during these saccades differed significantly between spontaneous (~12 degrees) and loom-evoked (~25 degrees) turns (Figure S1). To analyze the timing for flight turns of similar magnitude, but in different context, we increased the saccade detection threshold until average amplitudes become comparable between the two modes of flight turns. The timing analysis results were unaffected by this change of the threshold (Figures S1D and 4J).

For the analysis of movement-onset times for different body parts (Figure 4J), we first calculated a baseline value as the mean signal in the 50-ms window prior to saccade onset. We then calculated the peak value in the 500 ms after the saccade onset time for each variable. The onset-time threshold was set at 30% of the distance from the baseline value to the peak value. If the signal crossed this threshold multiple times, the final time that the signal crossed the threshold was defined as the 30%-amplitude crossing (i.e., signal onset) time (Figures 4H and 4J).

For the analysis of onset times for the saccade-related potentials (Figures 4C and 4D), we measured the baseline amplitude in the 50-ms window, starting 70 ms prior to saccade onset. This window ended 20 ms prior to the detected onset of the saccade because saccade-related potentials may start even before saccade onset, as detected in the L–R WBA signal.[6] The peak amplitude was measured as the minimum amplitude of the signal within the 200-ms window after saccade onset. A range of threshold values, from 10% to 50%, was then set from the baseline amplitude toward the peak amplitude for each signal. The onset latency was then measured for each fly's L–R WBA and *Vm* traces by calculating the time at which the signal crosses down a threshold amplitude for the last time, between the saccade onset and the peak. To estimate the 30-% onset latency, we calculated latency values for the range of threshold values and used their mean value as the 30-% onset latency. We used the same method for calculating the onset time of the "L–S" motor-related input curve in Figure 4B.

To test the effect of slow L-R WBA onset dynamics in optomotor trials compared to that of loom trials (Figure 5G), we selected 20 loom trials with the lowest onset slope and 20 optomotor trials with the highest onset slope. The onset slope was measured as a slope between two points within the onset slope of L–R WBA: 20-% and 80-% points between the baseline and the peak L–R WBA. The baseline was measured as the mean L–R WBA in the 100 ms immediately prior to the stimulus onset, and the peak amplitude was measured as the minimum L–R WBA within the 200 ms immediately after the stimulus onset.

Statistical analysis

Vm and L-R WBA traces in Figures 2 and 3 are represented as mean ± SEM. We tested for bimodality (Figure 3) using the UniDip test (https://github.com/BenjaminDoran/unidip).[20] Error bars on the bar plots in Figures 4, 5, S1, and S2 indicate 95% confidence intervals. Linear fits in Figures 2, 3, and 5 are calculated by the least-squares method. We used a paired t test to compare the amplitude and the time of L-R WBA, head and abdomen variables between different modes of flight turns in Figures 4, S1, and S2.